

A Phantom Menace?

Cosmological Consequences of a Dark Energy Component

with Super-Negative Equation of State

R. R. Caldwell¹

Department of Physics & Astronomy, Dartmouth College, Hanover, NH 03755

Abstract

It is extraordinary that a number of observations indicate that we live in a spatially flat, low matter density Universe, which is currently undergoing a period of accelerating expansion. The effort to explain this current state has focused attention on cosmological models in which the dominant component of the cosmic energy density has negative pressure, with an equation of state $w \geq -1$. Remarking that most observations are consistent with models right up to the $w = -1$ or cosmological constant (Λ) limit, it is natural to ask what lies on the other side, at $w < -1$. In this regard, we construct a toy model of a “phantom” energy component which possesses an equation of state $w < -1$. Such a component is found to be compatible with most classical tests of cosmology based on current data, including the recent type 1a SNe data as well as the cosmic microwave background anisotropy and mass power spectrum. If the future observations continue to allow $w < -1$, then barring unanticipated systematic effects, the dominant component of the cosmic energy density may be stranger than anything expected.

*Robert.R.Caldwell@dartmouth.edu

Arguments have been put forward that we live in a spatially flat, low matter density Universe which is currently undergoing a period of accelerating expansion. If the observational evidence upon which these claims are based are reinforced and strengthened by future experiments, the implications for cosmology will be incredible. It would then appear that the cosmological fluid is dominated by some sort of fantastic energy density, which has negative pressure, and has just begun to play an important role today. No convincing theory has yet been constructed to explain this state of affairs, although cosmological models based on a dark energy component, such as the cosmological constant (Λ) or quintessence (Q), are leading candidates. At this stage we are led to notice that the parameterization of the dominant energy component as a fluid with an equation of state (defined as the ratio of pressure to energy density) $w(\equiv p/\rho) \geq -1$ leads to the curious situation that most observational constraints are consistent with models that go right up to the $w = -1$ border [1]. It is natural to ask what lies on the other side of this boundary. The focus of this paper is the investigation of cosmological models with a dominant component for which $w < -1$.

We begin by constructing a classical cosmology: a spatially flat FRW space-time filled by a cold dark matter (CDM) component and a “phantom” (P) energy component. (A phantom is something which is apparent to the sight or other senses but has no corporeal existence – an appropriate description for a form of energy necessarily described by unorthodox physics, as will be seen later.) The phantom energy has positive energy density, $\rho_p > 0$, but negative pressure, such that $\rho_p + p_p < 0$. (It is no fatal flaw for a component to violate the dominant energy condition for a finite time, as can arise from a bulk viscous stress due to particle production [2].) It immediately follows from the equation of state $w < -1$ that the phantom energy density grows with time. If this energy has begun to dominate today, it must have come on like a bolt from the blue. Taking the constant value $w = -3$ as an example, then $\rho_p \propto a^6$ where a is the expansion scale factor. So if $\Omega_m \sim 0.3$ today, then the Universe contained 90% CDM at $z \sim 0.4$ as opposed to $z \sim 1.8$ in a Λ -dominated cosmology. Hence, the phantom energy exerts its influence very late. We now turn to quantify the remarkable

effect on the cosmology of a component with super-negative equation of state, $w < -1$.

The expansion scale factor grows rapidly when the phantom energy comes to dominate the Universe, as \dot{a}/a actually grows and the deceleration parameter $q_0 = (1 + 3w\Omega_p)/2$ becomes very negative. In fact, the scale factor diverges in finite time: if the expansion is matter dominated until the time t_m , then we can write the phantom energy-driven scale factor as $a(t) = a(t_m)[-w + (1+w)t/t_m]^{2/3(1+w)}$ at $t > t_m$. For $w = -3$ then a diverges when $t = 3t_m/2$. Unless $\Omega_m \ll 1$, however, $t_0 < t_m w/(1+w)$ and so the limiting cosmological time occurs well after the present day.

The expansion age, and similarly the horizon distance in a phantom energy cosmology are larger than in the analogous Λ model. In Figure 1 we show the age for a sequence of $w \leq -1$ models. In the range of interest, near $\Omega_m \sim 0.3 - 0.4$, we see that the phantom energy can increase the age by up to $\sim 30\%$ over the $w = -1$ age. For a given value of Ω_m , as w becomes very negative the phantom energy becomes important later and later with diminishing effect on the age. In fact, for $\Omega_m = 0.3$, the bound on the age in units of the Hubble time is $H_0 t_0 \leq 1.2$.

The volume - red shift relationship is demonstrated in Figure 2. For the same matter density, the phantom energy model gives the largest differential number of objects per red shift interval. Although evolutionary effects are important in cosmological tests based on this relationship, if all other features are held fixed, the phantom model will predict more strong gravitationally lensed quasars than Q or Λ models.

The magnitude - red shift relationship is demonstrated in Figure 3. The predictions for several cosmological models have been shown along with a summary of the observational results. All other parameters being equal, one expects high red shift supernovae to be dimmer in a phantom energy Universe.

Considering the constraint to the allowed range of w and Ω_m due to the supernovae, we find that phantom energy models even with very negative w are in accord with the observations. We see in Figure 4 that the contour region is extensive for $w < -1$, preferring a slightly higher matter density than in Quintessence models. An alternative way to visualize

this constraint on phantom models is to construct a parameter space in terms of the red shift at which the energy density drops to 90% matter, signalling the end of the matter-dominated epoch, rather than the constant equation of state w . The right-hand panel above makes clear that an important difference with other dark energy models is the very late onset of the phantom energy.

The next challenge is to construct a microphysical model of the phantom energy in order to consistently determine the impact on the cold dark matter, baryon, and photon fluctuation spectra.

We describe the system of gravitation, normal matter, and phantom energy with the Lagrangian $L = -R/16\pi G + L_m + L_p$ where L_m represents the Lagrangian for the “normal” matter, CDM plus the standard model particles and fields. Since it is not possible to achieve $w < -1$ with a free scalar field, and we wish to avoid interactions with other fields in order to keep the energy “dark,” we start with the unorthodox Lagrangian $L_p = -\partial_\mu\phi\partial^\mu\phi/2 - V(\phi)$ (with metric signature $+ - - -$). The important point is that we have switched the sign of the kinetic term in the scalar field Lagrangian L_p . In this way, $\rho_p = -\dot{\phi}^2/2 + V$ and $p_p = -\dot{\phi}^2/2 - V$ so that $w \leq -1$ is attained. The equations of motion are $\ddot{\phi} + 3H\dot{\phi} = +V_{,\phi}$, so that the field will tend to run up, not down, a potential towards larger energy. The key ingredient for this crude toy model, and the more detailed model we introduce later, is the non-canonical kinetic energy term, examples of which occur in supergravities [3] and in higher derivative theories of gravity [4].

The cosmological spectrum of fluctuations in the phantom field develop in a fashion similar to the case of Quintessence [5]. The Fourier transform of the linearized perturbation equation is $\ddot{\delta\phi} + 3H\dot{\delta\phi} + (k^2 - V_{,\phi\phi})\delta\phi = -\dot{h}\dot{\phi}/2$, where h is the synchronous gauge metric perturbation. In this equation, the sign of $V_{,\phi\phi}$ is different than in the standard case. Just as for Quintessence, perturbations on small scales, for $k^2 \gg |V_{,\phi\phi}|$, are suppressed. On larger scales, however, the phantom energy develops inhomogeneities in response to the surrounding matter and density perturbations. If the effective mass, $(k^2 - V_{,\phi\phi})^{1/2}$, should become imaginary then $\delta\phi$ would develop a growing (tachyon) instability. However, if we

implement a constant equation of state, then $V_{,\phi\phi} = \frac{3}{2}(1-w)[\dot{H} - \frac{3}{2}H^2(1+w)]$, which is negative for a limited range of values of w and Ω_m . Consequently, the effective mass is real, and there is no instability for constant w .

A more versatile phantom model can be constructed using a Lagrangian with a non-standard dependence on the field gradients, $L_p = a(\phi)(\nabla\phi)^2 + b(\phi)(\nabla\phi)^4 + \dots$, motivated by the appearance of higher derivatives in string theory. This approach has been employed in the k-inflation and k-essence scenarios [6,7,8], and it has been demonstrated [6,9] that such models can also be used to describe an energy component with a super-negative equation of state, $w_p < -1$, which is also stable to perturbations (no tachyonic instability). Details of the treatment of cosmological perturbations in the k-essence scenario are given in [10]; the approach is sufficiently general that the case of a phantom is simply accommodated. Hence, starting from a theory giving the functional dependence of L_p on ϕ and $(\nabla\phi)^2$, one can readily determine the stress-energy $\rho(z)$, $p(z)$ and the sound speed of perturbations $c_p(z)$ as they evolve in time or red shift.

Turning this around, one may instead dictate the histories $w_p(z)$ and $c_p(z)$ in order to specify the phantom dark energy model. In the present investigation we focus on constant- w_p and $c_p = 1$ models. Although this is not a generic prediction of the dynamical models described above, the observational differences are not expected to be very large (as some exploratory analyses have confirmed). Since the observational effects rely on a substantial fractional phantom energy density, and since $\rho(z)$ is actually growing with time, then the relevant values of $w_p(z)$ and $c_p(z)$ are the mean values between the redshift when the phantom began to dominate and the present. For $w_p < -1$, this is a narrow range in redshift, leaving little opportunity for the effects of time-variation to be distinct. As we have modified CMBfast [11] to include a phantom dark energy component based on both approaches, we now proceed to discuss the resulting perturbation spectra.

The main feature that distinguishes the phantom energy case from Λ or Q is that the onset of phantom energy dominance happens at the very last moment – so late that most

evolutionary effects which occur in Λ and Q models are suppressed. In the cases illustrated in Figure 5 the strength of the late-time ISW effect diminishes as w becomes more and more negative, because the expansion is CDM-dominated until later and later. On small angular scales the locations of the acoustic peaks shift to higher multipole moments as w becomes more negative, due to the increased distance to the last scattering surface. This may be an important factor in attempts to develop a phantom dark energy cosmological model to accommodate the newer CMB results, also represented in Figure 5. A more detailed analysis will be forthcoming.

The phantom-dominated background evolution has an important effect on the fluctuation spectra, as well. Making the assumptions that the matter component of the cosmological fluid carries a spectrum of scale-invariant perturbations generated by inflation, and that, similar to Quintessence, the phantom energy itself does not fluctuate on scales well below the Hubble horizon, then we may follow the growth of linear perturbations in the CDM and baryons. The growth suppression factor $g = D(a)/a$ is shown in Figure 6, where we see that perturbations grow as $D \propto a$ until very late, owing to the very late time at which the phantom energy begins to dominate. Hence, the evolution is very similar to the standard CDM scenario, but with a lower matter density.

Next, we consider the behavior of the mass power spectrum for $w < -1$. Because the phantom field does not fluctuate on scales well below the horizon, the overall shape of the mass power spectrum is well-described by the BBKS parameterization [12]. (See [13] for instructions on how to adapt the fitting functions to quintessence). The normalization is obtained by comparison with the CMB. Using the amplitude of the first acoustic peak, then the normalization is similar to a Λ CDM model with the same cosmological parameters, but with a σ_8 higher by a ratio of the growth suppression factors g_P/g_Λ . Since $g_\Lambda(\Omega_m = 0.35, a = 1) = 0.8$, and g_P is at most unity in the limit of $w \ll -1$, then σ_8 is higher by up to 20%. Using COBE for the normalization, on the other hand, the effect of the late ISW and the direct fluctuations in the phantom field must also be taken into account. However, owing to the late onset of the phantom, there is very little late ISW and the direct fluctuations are

also negligible. As mentioned earlier, the low- ℓ spectrum is very flat, as in SCDM, and up to $\sim 5\%$ lower than in the comparable Λ CDM model. Hence, the COBE normalized spectrum will result in a power spectrum with a σ_8 up to $\sim 20 + 5\%$ higher than for Λ .

In Figure 7 we show the prediction and observational constraint on σ_8 for a sequence of models varying in w . While the amplitude of the CMB-normalized mass power spectrum grows slightly as w becomes more negative, the implied σ_8 based on the observed abundance of clusters grows as well. (The cluster abundance calculation is based on an extension of [14] to the case of $w < -1$.) We see that the intersection of the 2σ regions of σ_8 grows with decreasing w . Further constraints based on large scale structure one may consider, but which are beyond the scope of this paper, include the evolution of the abundance of rich clusters and the growth rate of the linear fluctuation spectrum. Our lesson here is that phantom dark energy models do exist which, upon first inspection, satisfy constraints based on the CMB and the mass power spectrum.

In summary, we have investigated the properties of cosmological models in which the dominant energy density component today has an equation of state $w < -1$. We have demonstrated the impact on the cosmological age, the volume - red shift and magnitude - red shift relations, the CMB, and the mass power spectrum, finding broad agreement with current observational constraints. Current data appears to be consistent with a phantom, although a more careful analysis will be necessary to quantify the observational status of $w < -1$.

While there is no single, best method for determining if the equation of state is strongly negative, combinations of measurements of the type described in this paper will substantially improve our understanding of the dark energy. One of our central points is the importance that such analyses are open to the possibility of a phantom dark energy – unjustified biases and priors can lead to a gross misinterpretation of the observational evidence. (See [15] for an analysis of the pitfalls of assuming a constant w or $w \geq -1$.)

Of course, we do not want to overlook the distinct possibility that the observational evidence in favor of such a strongly negative equation of state is simply a phantom – that the

apparent accelerating expansion is due to more conventional, though unanticipated causes (*e.g.* dust or evolution for the SNe). If these systematic effects can be eliminated, and the data continue to support $w < -1$ then the implications for fundamental physics would be astounding, since $w < -1$ cannot be achieved with Einstein gravity and a canonical Lagrangian. It is premature to shift attention towards building $w < -1$ models, but it is important to be aware of the properties and implications of models in each direction of the cosmological parameter space.

As has been discussed elsewhere, current observations suggest the presence of a dark energy component with $w \lesssim -0.5$ [1], with many constraints pushing towards $w = -1$: the observations are teetering at the edge of a previously unfamiliar boundary.

ACKNOWLEDGMENTS

The SNe data used in Fig 3 were obtained from Adam Riess [16]. The cluster abundance constraint in Figure 7 was evaluated by Limin Wang. This work was supported by the US DoE grant DE-FG02-91ER40671 (at Princeton) and the NSF grant PHY-0099543 (at Dartmouth).

REFERENCES

- [1] Wang, L., Caldwell, R.R., Ostriker, J., & Steinhardt, P.J., *Astrophys. J.* 530, 17 (2000).
- [2] Barrow, John D., *Nucl. Phys. B* 310, 743 (1988).
- [3] Nilles, H.P., *Phys. Rep.* 110, 1 (1984).
- [4] Pollock, M.D., *Phys. Lett. B* 215, 635 (1988).
- [5] Caldwell, R.R., Dave, R. & Steinhardt, P.J., *Phys. Rev. Lett.* 80, 1586 (1998).
- [6] Armendariz-Picon, C., Damour, T., & Mukhanov, V., *Phys. Lett. B* 458, 209 (1999).
- [7] Armendariz-Picon, C., Mukhanov, V., & Steinhardt, P.J., *Phys. Rev. Lett.* 85, 4438 (2000).
- [8] Armendariz-Picon, C., Mukhanov, V., & Steinhardt, P.J., *Phys. Rev. D* 63, 103510 (2001).
- [9] Chiba, T., Okabe, T., & Yamaguchi, M., *Phys. Rev. D* 62, 023511 (2000).
- [10] Erickson, J.K. *et al.*, *Phys. Rev. Lett.* 88, 121301 (2002).
- [11] Seljak, U. & Zaldarriaga, M., *Astrophys. J.* 469, 437 (1996).
- [12] Bardeen, J.M., Bond, J.R., Kaiser, N., & Szalay, A.S., *Astrophys. J.* 304, 15 (1986).
- [13] Ma, C.-P., Caldwell, R.R., Bode, P. & Wang, L., *Astrophys. J.* 521, L1 (1999).
- [14] Wang, L. & Steinhardt, P.J., *Astrophys. J.* 508, 483 (1998).
- [15] Maor, I., Brustein, R., McMahon, J., & Steinhardt, P.J., *astro-ph/0112526* (2001).
- [16] Riess, Adam G., private communication (2002).
- [17] Riess, Adam G. *et al.*, *Astronom. J.* 116, 1009 (1998).
- [18] Perlmutter, S. *et al.*, *Astrophys. J.* 517, 565 (1999).
- [19] Riess, Adam G. *et al.*, *Astrophys. J.* 560, 49 (2001).

[20] Wang, X., Tegmark, M., & Zaldarriaga, M., astro-ph/0105091 (2001).

FIGURES

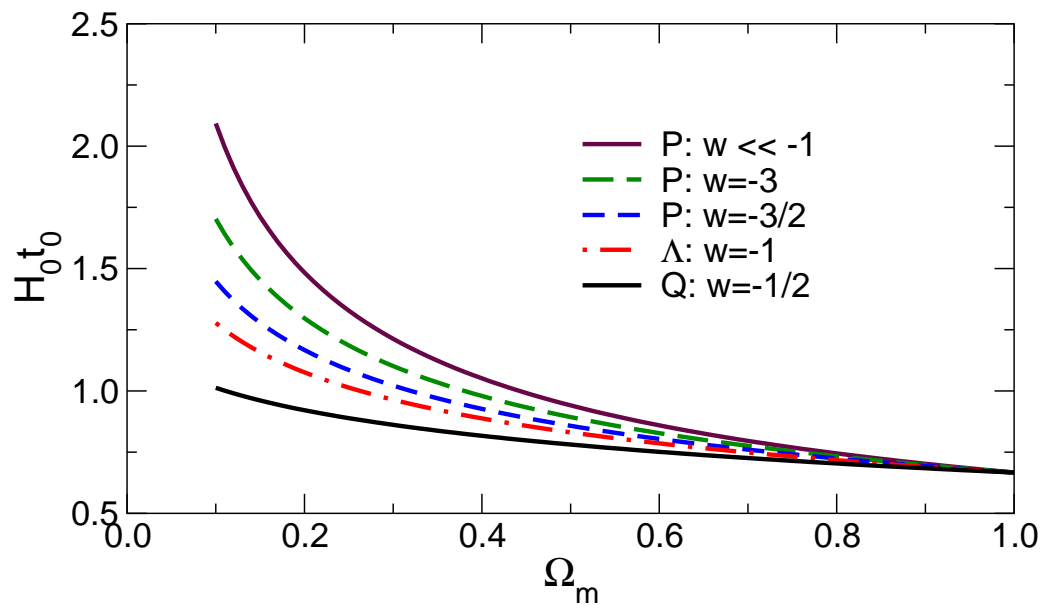


FIG. 1. The age in units of the Hubble time is plotted versus Ω_m for a series of cosmological models containing dark energy with different values of w .

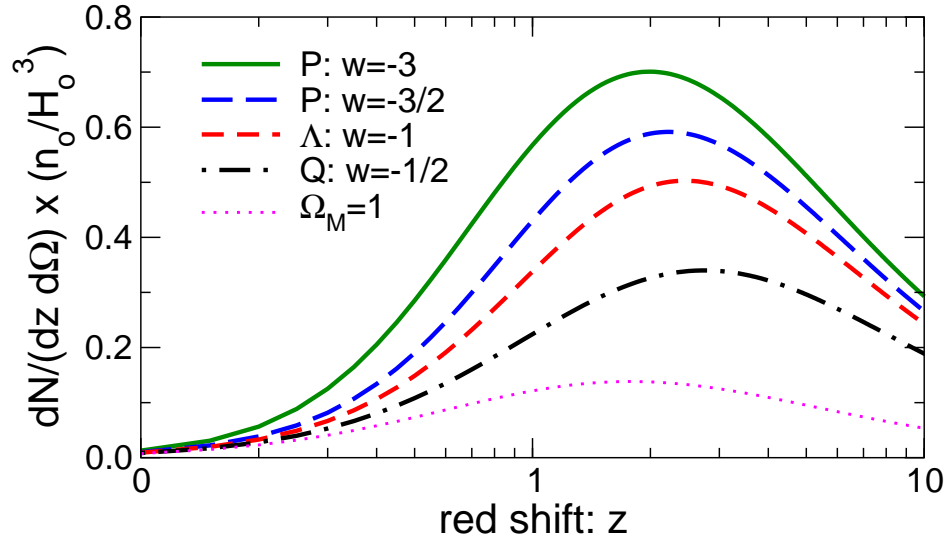


FIG. 2. The volume - red shift relationship is shown for phantom energy models with $w = -3, -3/2, \Lambda$ CDM with $w = -1$, QCDM with $w = -1/2$, and CDM. All the dark energy models have $\Omega_m = 0.3$.

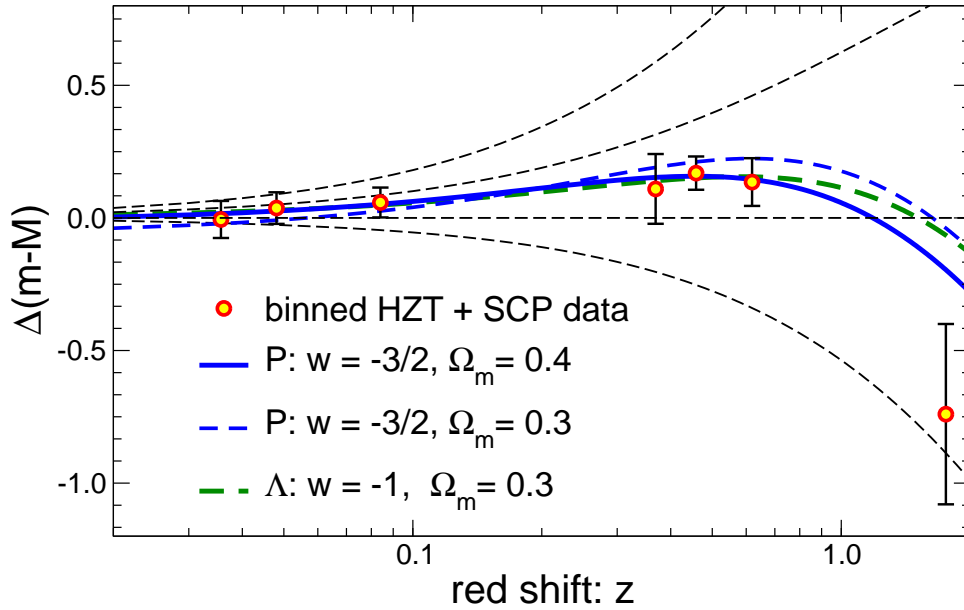


FIG. 3. The magnitude - red shift relationship is shown for the redshift-binned type 1a SNe data (HZT- [17]; SCP- [18]; binning- [19]), alongside the predictions of various cosmological models. Both the phantoms ($w = -3/2, \Omega_m = 0.4; -3/2, 0.3$) and the Λ model ($-1, 0.3$) provide good fits to the data (low $\chi^2/\text{d.o.f.}$). The magnitudes are calculated relative to an empty, open Universe. The light, dashed lines are for pure phantom, deSitter, Milne, and Einstein-deSitter, from top to bottom.

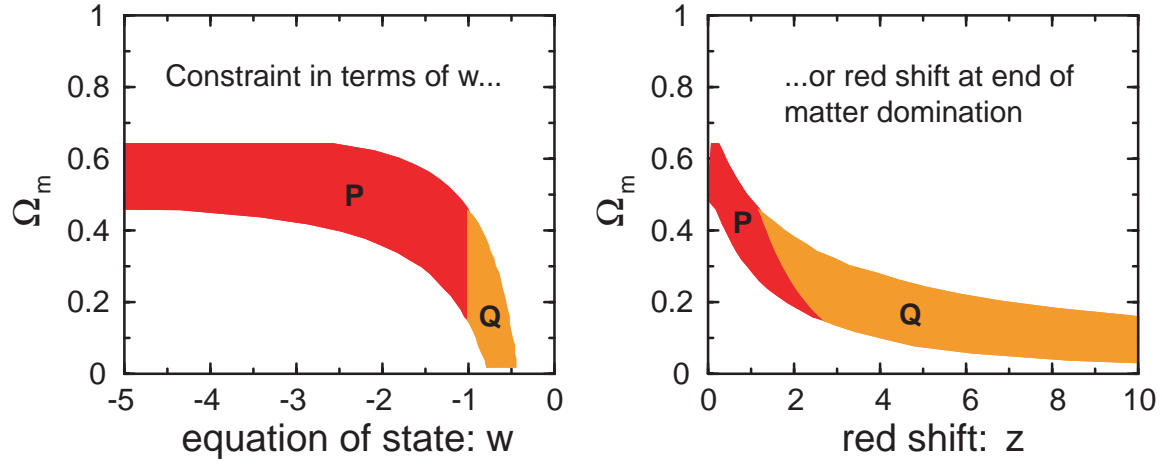


FIG. 4. The constraint on the allowed values of Ω_m in phantom and quintessence dark energy models is shown as a function of w , or alternatively the red shift at which matter-domination ends, when $\Omega_m = 0.9$. We have traversed the $w = -1$ boundary, finding that there are phantom energy models in accord with the observations.

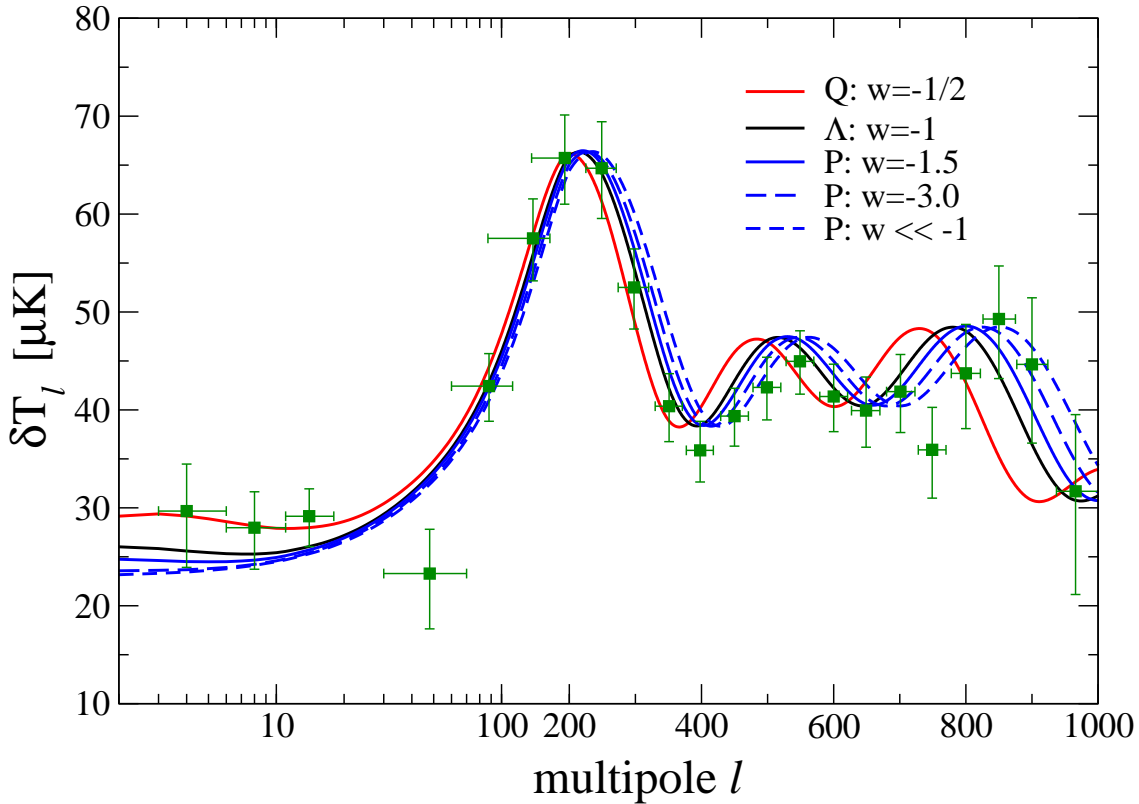


FIG. 5. The CMB anisotropy spectra are shown for various cosmological models with equal input power, to demonstrate the effect of $w < -1$. On large angular scales, the strength of the late-time ISW effect diminishes as w becomes more and more negative, because the expansion is CDM-dominated until later and later. The locations of the acoustic peaks shift to smaller angular scales as w becomes more negative, due to the increased distance to the last scattering surface. The models shown all have $\Omega_m = 0.35$, $\Omega_b h^2 = 0.02$, and $h = 0.70$. The horizontal axis is logarithmic for $2 < l < 200$ in order to give enough space to both large and small angular scale features. Comparing the curves with a compilation of current CMB data [20] suggest a more negative dark energy equation-of-state may allow for a better fit to the small angular scale data.

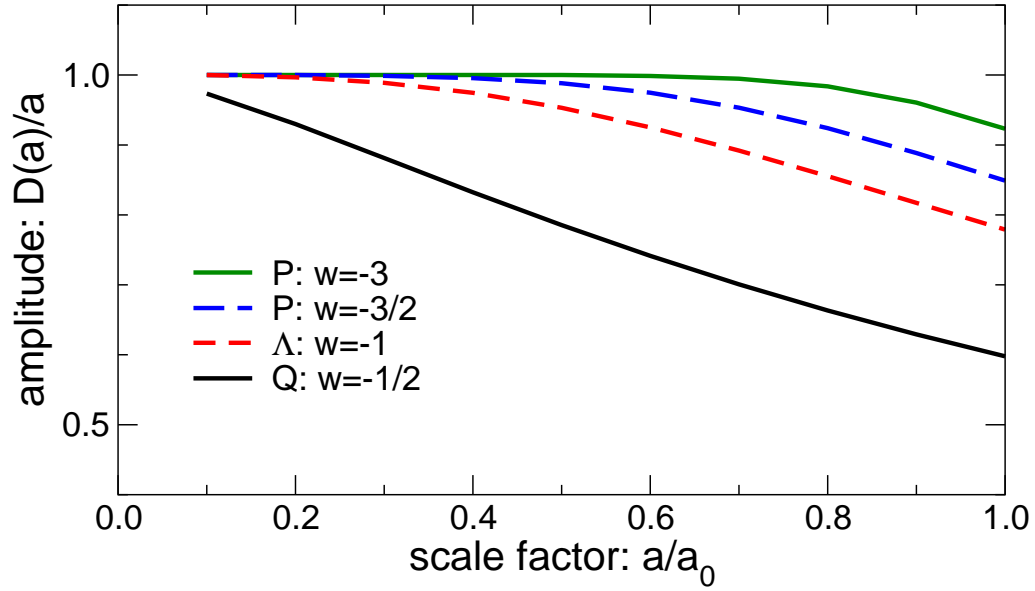


FIG. 6. The amplitude of the growth suppression factor $g = D(a)/a$ versus the scale factor is shown for various cosmological models. We see that the perturbation growth is slowed later, with weaker effect, in the phantom energy models. The models shown all have $\Omega_m = 0.3$. For SCDM, $D(a)/a = 1$.

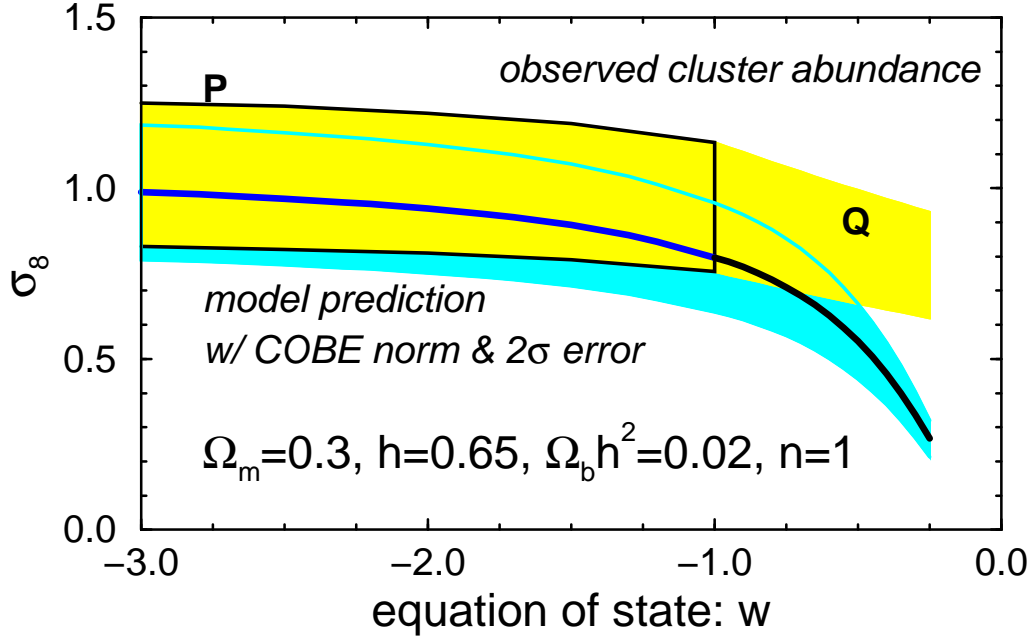


FIG. 7. The cluster abundance constraint is shown for a sequence of Q ($w > -1$), Λ ($w = -1$), and phantom ($w < -1$) models with $\Omega_m = 0.3$, $h = 0.65$, $\Omega_b h^2 = 0.02$, $n = 1$. The upper shaded region shows the 2σ range of σ_8 based on the observed abundance of x-ray clusters, as interpreted for a range of w (based on an extension of the work in Ref. [14]). The lower shaded region shows the predicted σ_8 for COBE-normalized models. The intersection of the two regions grows as w becomes more negative. The letters P and Q indicate the Phantom and Quintessence regions, to the left and right of $w = -1$.